Pathogenesis of *Borrelia burgdorferi* and *Babesia microti* in TLR4-Competent and TLR4-dysfunctional C3H Mice

Lavoisier Akoolo[#1], Vitomir Djokic[#1], Sandra C. Rocha[1], Nikhat Parveen[1]

[1]Department of Microbiology, Biochemistry and Molecular Genetics, Rutgers New Jersey Medical School, Newark, NJ, USA

[#] These authors contributed equally to this work.

Summary

Toll-like receptors (TLRs) are a class of membrane-spanning proteins of host cells. TLR2 and TLR4 are displayed on the surface of macrophages, neutrophils and dendritic cells and recognize structurally conserved microbial signatures defined as Pathogen associated molecular patterns (PAMPs). C3H mice are susceptible to tick-borne pathogens; Lyme disease causing *Borrelia burgdorferi* that manifests arthritis and carditis and Apicomplexan protozoan, *Babesia microti* (*Bm*) that causes significant parasitemia associated with erythrocytopenia and haemoglobinuria. *B. burgdorferi* lacks typical TLR4 ligand lipopolysaccharides (LPS) and *Bm* TLR ligand(s) remain unknown. Only *Borrelia* lipoproteins that signal through TLR2 are established as PAMPs of these pathogens for TLR2/TLR4. Infection of C3H mice with each pathogen individually resulted in increase in the percentage of splenic B, T, and FcR+ cells while their co-infection significantly diminished levels of these cells and caused increased *B. burgdorferi* burden in the specific organs. The most pronounced inflammatory arthritis was observed in co-infected C3H/HeJ mice. Parasitemia levels and kinetics of resolution of *Bm* in both mice strains were not significantly different. Transfected HEK293 cells showed pronounced signaling by *B. burgdorferi* through TLR2 and to some extent by TLR4 while *Bm* and infected erythrocytes did not show any response confirming our results in mice.

Graphical Abstract

TLR4 stimulation in C3H/HeN mice by *B. burgdorferi* by unknown (indicated by a question mark) ligand(s) early in infection causes suppression of TLR2 expression. An increase in TLR2 expression in C3H/HeJ mice in the absence of a functional TLR4 possibly enhances signaling by

---

Tri-Acylated lipoproteins of colonized *B. burgdorferi* resulting in an increase in inflammatory Lyme arthritis, particularly during co-infection that is associated with higher lymphocytes infiltration and hyperplasia of synovium in *B. burgdorferi* infected, and co-infected C3H/HeJ mice. *In vitro* TLR2 signaling by Lyme spirochetes, and the lack of signaling through TLR2/TLR4 by egressed *Bm* or iRBCs (marked by a cross) support this model.

Keywords

Babesia microti ; *Borrelia burgdorferi* ; Lyme disease; Babesiosis; Co-infection; Inflammation; Toll like receptor 4

INTRODUCTION

Lyme disease is the most prevalent tick-borne infection in Europe and North America. The CDC estimates that 300,000 to >400,000 cases of Lyme disease and ~2000 cases of human babesiosis occur in the USA annually and Lyme spirochetes infect ~65,000 people in Europe every year (Fallahi, Elia, & Bonatti, 2017; Kugeler, Schwartz, Delorey, Mead, & Hinckley, 2021). *Borrelia burgdorferi* infection could result in systemic Lyme disease that affects skin, musculoskeletal system, heart, joints and neuronal system (Steere, 2001). *Babesia microti* (*Bm*) and *B. divergens* are the major cause of babesiosis in the USA and Europe, respectively. *Babesia* species are intraerythrocytic tick-borne Apicomplexan protozoan parasites that cause increased lysis of red blood cells that is associated with anemia, jaundice and splenomegaly (Homer, Aguilar-Delfin, Telford, Krause, & Persing, 2000). Healthy individuals infected with *Bm* remain asymptomatic such that transfusion of donated blood of these people to immunocompromised recipients often leads to transfusion-associated babesiosis and results in high morbidity and mortality (Herwaldt et al., 2011; Krause et al., 2008; Krause et al., 1998).

Co-infections of *Ixodes* species ticks with *B. burgdorferi* and *Bm* have been increasing steadily over the years (Hersh et al., 2014; Lommano, Bertaiola, Dupasquier, & Gern, 2012; Moutailler et al., 2016; Piesman et al., 1986; Schulze, Jordan, Healy, & Roegner, 2013). The same reservoir host(s) and tick vector feeding habits determine the spread of these pathogens to humans (Swanson, Neitzel, Reed, & Belongia, 2006). Although co-infections with various tick-borne pathogens have also been increasing in humans in regions of North America and Europe (Aliota et al., 2014; Caulfield & Pritt, 2015; Hersh et al., 2014; Horowitz et al., 2013; Jahfari et al., 2016; Moutailler et al., 2016; Panczuk, Tokarska-Rodak, Koziol-Montewka, & Plewik, 2016; Primus et al., 2018; Schlachter, Chan, Marras, & Parveen, 2017; Tomasiewicz, Chmielewska-Badora, Zwolinski, & Murias-Brylowska, 2016), the most common co-infections in the Northeastern United States occur with *B. burgdorferi* and *Bm*, accounting for ~80% of tick-borne concurrent infections by these pathogens (Swanson et al., 2006). Co-infections with *Babesia* species and Lyme disease causing *B. burgdorferi* sensu lato group of spirochetes are also emerging as a serious problem in Europe in addition to the United States (Diuk-Wasser, Vannier, & Krause, 2016; Dunn et al., 2014; Knapp & Rice, 2015; Rizzoli et al., 2014). Epidemiological studies demonstrate that *Bm-B. burgdorferi* co-infected patients exhibit persistence of more diverse and intense symptoms (Krause et al.,

2003; Krause et al., 2002; Krause et al., 1996). Therefore, a comprehensive evaluation of the effect of co-infections on overall disease severity affected by host factors remains a great urgency.

Early murine model studies showed contradictory outcomes of *Bm-B. burgdorferi* co-infections as relevant to severity of Lyme disease (Coleman, LeVine, Thill, Kuhlow, & Benach, 2005; Moro et al., 2002). Susceptibility of the host and pathogenicity of infection depends on virulence factors of microbes and the genetic background of the host with respect to the modulating effect of the immune system (Benoit et al., 2010; Gronberg-Hernandez, Sunden, Connolly, Svanborg, & Wullt, 2011; Wells et al., 2003). To address the effect of selected mouse strain on infection with tick-borne pathogens (S. W. Barthold, Beck, Hansen, Terwilliger, & Moody, 1990; Borggraefe et al., 2006; Coleman et al., 2005; Vannier et al., 2004), we were prompted to use two different derivatives of C3H mice to investigate the pathogenesis of *B. burgdorferi* and *Bm*. Similar to other pathogens, infection of the host by *Bm* and *B. burgdorferi* triggers an early innate immune response that is usually initiated by recognition of pathogen-associated molecular patterns (PAMPs) through responsive pattern recognition receptors (PRRs) in host cells that provides the first line of defense against invading pathogens (Baravalle et al., 2010; Bose, 1994; W. C. Brown, Norimine, Knowles, & Goff, 2006; Bulut, Faure, Thomas, Equils, & Arditi, 2001; Cervantes et al., 2011; Love, Schwartz, & Petzke, 2014; Oosting et al., 2010; Rahman, Shering, Ogden, Lindsay, & Badawi, 2016; Suarez et al., 2011; Werling & Jungi, 2003; Wooten et al., 2002a, 2002b). PAMPs-mediated signaling through PRRs is crucial for many aspects of microbial pathogenesis such as recruitment of inflammatory cells to the infected tissue, expression of pro-inflammatory mediators, modulation of innate and adaptive immunity and eventual clearance of infecting organisms. Excessive activation of PRRs is harmful with a significant pathology caused by systemic or localized inflammation in hosts (Heine & Lien, 2003; Takeuchi & Akira, 2010) and can lead to chronic disease or death.

Mating of female BALB and male DBA mice resulted in the development of the current inbred C3H strain. The C3H strain was introduced to the Charles River and Jackson Laboratory in 1970s. Expression of PRRs may differ across host genetic background causing varying degrees of pathogenicity by the infecting microbe to affect disease severity (S. W. Barthold et al., 1990; Borggraefe et al., 2006). A classic case of differing expression of Toll Like Receptor 4 (TLR4) in the same genetic background are the C3H/HeN mice that retain a functional TLR4 receptor, and the C3H/HeJ mice in which a spontaneous point mutation in the TLR4 gene *Tlr4^{Lps-d}* rendered it dysfunctional (Totemeyer, Foster, Kaiser, Maskell, & Bryant, 2003). In the United States, the suppliers Charles River and Jackson Laboratory offer either C3H/HeN or C3H/HeJ strains but not both. Both C3H/HeN and C3H/HeJ mice are susceptible to infection with *B. burgdorferi*, and manifest severe lesions like polyarthritis and carditis (Armstrong, Barthold, Persing, & Beck, 1992; S.W. Barthold, 1991; G. Wang et al., 2001). These strains of mice are also susceptible to *Bm* and exhibit pronounced parasitemia, anemia and splenomegaly similar to that observed in humans (Coleman et al., 2005; V. Djokic, Akoolo, L., Primus, S., Schlachter, S., Kelly, K., Bhanot, P., and N. Parveen., 2019; Djokic V, 2018). The most established PAMP recognized by TLR4 receptor is lipopolysaccharide (LPS), a component of the outer membrane of Gram-negative bacteria. TLR4/myeloid differentiation factor 2 (MD-2) complex recognizes LPS to induce

an innate immune response (Chow, Young, Golenbock, Christ, & Gusovsky, 1999; Nagai et al., 2002; Schromm et al., 2001; Shimazu et al., 1999; Y. Wang et al., 2016). Therefore, it is not surprising that the C3H/HeJ mice are more susceptible to infections with several Gram-negative bacteria such as *E. coli* and *S. typhimurium* (Hagberg, Briles, & Eden, 1985; Hagberg et al., 1984). *B. burgdorferi* outer membrane lacks classical LPS, and hence does not typically stimulate a typical TLR4 mediated immune response (Takayama, Rothenberg, & Barbour, 1987); however, *B. burgdorferi* expresses a large number of lipoproteins that contribute to the major inflammatory pathway by activating monocytes∕macrophages, neutrophils, dendritic cells, lymphocytes, endothelial cells and fibroblasts through TLR2 signaling (Cervantes et al., 2011; Gautam et al., 2012; Lasky, Pratt, Hilliard, Jones, & Brown, 2016; Lien et al., 1999; Liu, Montgomery, Barthold, & Bockenstedt, 2004; Lorenz, Mira, Cornish, Arbour, & Schwartz, 2000; Morr, Takeuchi, Akira, Simon, & Muhlradt, 2002; Rupprecht et al., 2007; Salazar et al., 2009; Salazar et al., 2005; Wooten et al., 2002a; Wooten & Weis, 2001).

Glycosylphosphatidylinositol (GPI) anchor on merozoites surface of a *Bm* related Apicomplexan parasite belonging to *Plasmodium* species have been reported to signal through both TLR2 and TLR4 that depends on GPI composition and could contribute to severe, cerebral and placental malaria (Gowda, 2007; Mockenhaupt et al., 2006a, 2006b; Seixas, Moura Nunes, Matos, & Coutinho, 2009). Only limited information is available for GPI anchored merozoite proteins of *Babesia* species and was reported not to induce stimulation of pro-inflammatory cytokines (Debierre-Grockiego et al., 2019; Delbecq et al., 2002; Nathaly Wieser, Schnittger, Florin-Christensen, Delbecq, & Schetters, 2019). The role of TLR4 in other protozoan parasites' pathogenesis (Campos et al., 2001; Debierre-Grockiego et al., 2007) led us to hypothesize that *Bm*'s GPI anchors can potentially also cause TLR4 and/or TLR2 stimulation. Unlike *Plasmodium* species and other protozoa, GPI composition in *Bm* proteins is not yet described, such that contribution of TLR2 and TLR4 for *Bm* remains to be investigated.

Our extensive analysis of the splenic immune response in young and older C3H/HeJ mice infected with *Bm, B. burgdorferi,* or co-infected with both pathogens at early (pre-peak parasitemia) stage of infection suggested that stimulation of innate immune response by *B. burgdorferi* likely causes reduction in peak parasitemia in the co-infected mice (V. Djokic, Primus, Akoolo, Chakraborti, & Parveen, 2018). An obvious question arose whether *Bm* and *B. burgdorferi* infections separately, or together in non-functional TLR4 containing C3H/HeJ versus conventional TLR4 possessing C3H/HeN mice show different host responses and respective disease manifestations. Following infection with *Bm*, the first line of defense is mediated by macrophages, producing TNF-$_\alpha$, and by NK cells reactive oxygen species and nitric oxide, and IFN-$_\gamma$ (Homer et al., 2000). Control of *Bm* infections at early and later stage is facilitated by activation of IFN-$_\gamma$ producing CD4 T cells that enhances killing of *Babesia* species by macrophages (V. Djokic et al., 2018; Igarashi et al., 1999; Skariah et al., 2017). Co-infection with *B. burgdorferi* and *Bm* results in exacerbation of Lyme disease manifestations in patients (Krause et al., 1996) but host factors involved in this enhancement in humans have not been assessed until now. In this study, we investigated the impact of signaling in the presence, or absence of functional TLR4 on the pathogenesis of *B. burgdorferi* and *Bm* infections individually, and during co-infections in C3H mice. We

further confirmed these results and determined contributions of TLR2 and TLR4 signaling by each pathogen individually using the transfected human embryonic kidney (HEK) 293 cells *in vitro*.

MATERIALS AND METHODS

Animal studies

The Newark Institutional Animal Care and Use Committee (IACUC) reviewed and approved the protocol number D-14011-A1 under which this study was conducted at Rutgers University New Jersey Medical School. Guidelines of the Animal Welfare Act, The Institute of Laboratory Animal Resources Guide for the Care and Use of Laboratory Animals, and Public Health Service Policy were followed in this study.

Culture and maintenance of *B. burgdorferi* and *Bm*

Bm (ATCC30221) was first inoculated in C3H severe combined immunodeficient (SCID) mice to obtain inoculum for subsequent experiments. To determine parasitemia, a drop of blood sample was collected from the infected mouse by tail bleed to prepare a smear. Thin blood smears were air-dried, fixed with absolute methanol for approximately five minutes and then stained using Giemsa solution diluted 1:2 in water for 15 minutes. To estimate parasitemia, Giemsa stained blood smears were examined under a light microscope and the number of infected red blood cells counted in a total of 20 to 50 fields at high magnification (10x and 100x ocular magnification oil immersion objective lenses). Parasitemia was expressed as a percentage of infected erythrocytes among total red blood cells counted. Bioluminescent *B. burgdorferi* N40 strain (N40 D10/E9 clone derivative) carrying a firefly luciferase gene (Bbluc) was used in this study (K. Chan, Alter, L., Barthold, S. W., and Parveen, N., 2015). Spirochetes were cultured at 33°C in Barbour-Stoenner-Kelly-II (BSK-II) medium supplemented with 6% rabbit serum (BSKII-RS).

Infection of mice with *B. burgdorferi* and *Bm*

Three-week old C3H/HeN and C3H/HeJ mice were purchased from reputed vendors (Charles River and Jackson, respectively) and after acclimatization for one-week, 35 mice of each strain were randomly divided into four experimental groups. A group of five mice of each strain was kept uninfected, and ten mice were used for each infection group. One experimental group of each mouse strain was injected with *B. burgdorferi* N40 alone, second group received both *B. burgdorferi* and *Bm* and third group was inoculated with *Bm* alone. To infect mice for experimental purpose, blood was collected from infected SCID mice and the number of parasitized RBCs calculated, as described above. Briefly, total number of RBCs per ml was determined using a hemocytometer. The number of infected RBCs was then determined by multiplying percent parasitemia with calculated total RBCs per ml of blood. The number of parasitized RBCs was then adjusted to 10^5 per ml in 1xPBS and 100μl injected in each mouse intraperitoneally (i.p.), i.e., 10^4 infected Red Blood Cells (iRBCs) inoculated per mouse. The spirochete numbers were adjusted to 10^4 per ml of medium and 100μl (10^3 *B. burgdorferi*) of inoculum was used for injection of each mouse subcutaneously (s.c.) on the dorso-lateral aspect of the right thigh. Our previous studies showed that subcutaneous injection of *B. burgdorferi* suspended in BSKII-RS allows

sufficient time for live-imaging of mice (K. Chan, Alter, L., Barthold, S. W., and Parveen, N., 2015). Since BSKII-RS may affect *Bm* adversely, we used different sites of infection for these pathogens such that consistent infection dose with healthy pathogens is ensured. Thus, we were able to conduct a well-controlled study with fewer variables introduced, which is not possible when natural, tickborne infection procedure is employed.

Monitoring of infected mice

Infected mice were monitored closely for both *B. burgdorferi* and *Bm* infection progression for up to 21 days post-infection, after which they were euthanized and evaluated for tissue colonization and disease pathology. Mice infected with *Bm* were monitored for parasitemia regularly by examination of Giemsa stained blood smears. Colonization by bioluminescent *B. burgdorferi* was monitored by live imaging at two and three weeks of infection using In Vivo Imaging System 200 (IVIS-200, Perkin Elmer, MA) and images captured. Briefly, after isoflurane anesthesia, each mouse was injected with $200_\mu l$ PBS containing 30mg/ml of D-luciferin intraperitoneally. Images were captured with three minutes exposure. At each stage, five uninfected mice were also imaged as controls for bioluminescence quantification after injection of the substrate and net radiance reported for infected mice was determined after deduction of average value from these controls (483.23 $p/s/cm^2/sr$). After 21 days of infection, mice were imaged, heparinated blood collected by cardiac puncture and animals were then euthanized. Plasma was recovered for antibody response determination.

Analysis of tissue colonization and disease pathology

To eliminate microbiome on skin surface, mice were soaked in Betadine for 30–40 minutes followed by submersion in 70% ethyl alcohol for 30 minutes and then dissected in biosafety hood and organs removed aseptically. The skin at the injection site, ear, and urinary bladder were transferred to tubes containing BSK-II+RS medium and antibiotic mixture allowing Borreliae (Sigma-Aldrich, MO) growth and restricting contaminants growth. *B. burgdorferi* were allowed to grow at 33°C to recover live spirochetes to ensure that tissue colonization has occurred by N40 strain. Cultures were monitored for up to 14 days and live spirochetes observed by dark field microscopy. DNA was isolated from the left hind leg, whole brain and heart together with major vasculature (aorta and left vena cava) and used for PCR quantification for *B. burgdorferi recA* amplicon using the specific molecular beacon probes tagged with FAM fluorophore in the duplex assay developed in our laboratory (K. Chan, Marras, & Parveen, 2013). Mouse DNA was quantified by determining nidogen amplicon copy number using the specific molecular beacon tagged with TET fluorophore for normalization of *B. burgdorferi* copy number to calculate relative spirochetes burden in each organ. Aseptically removed spleens were used to isolate splenocytes for flow cytometry.

Histopathology

Right hind legs of infected mice were fixed in 10% neutral buffered formalin for at least 48 hours after which bone tissue in joints was decalcified by 10% EDTA-decalcification protocol. Then, 5μm thick sections were cut by microtome, mounted on slides and stained with hematoxylin and eosin. Histopathological examination of sections of the tibiotarsus joint and knee were independently conducted in a blinded manner and scored according to the established criteria.

Isolation of T cells and Flow cytometry

Spleens were aseptically harvested from infected mice, weighed and single cell suspensions of the splenocytes obtained by slicing the organ into small pieces and straining into 50 ml conical tubes through a 70μm nylon sterile cell strainer. The cells were then washed with PBS by centrifugation at 1,500 rpm and RBCs lysed by Ammonium-Chloride–Potassium (ACK) lysis buffer (Thermofisher #A10492201). The splenocytes were resuspended in FACS buffer (PBS +5%FBS) at 10^6 cells/ml and labeled. Total splenocytes population was incubated for 30 minutes in the dark at 4°C in order to label B cells with Brilliant violet 421 conjugated anti-mouse CD19 antibodies (Bio legend, #115537), macrophages with BV605 conjugated anti-mouse F4/80 antibodies (Bio legend, #123133), all FcR+ cells with APC-Cy7 conjugated anti-mouse NK1.1 antibodies (Bio legend #108724), T cells with PE-Cy7 conjugated anti-mouse CD3 antibodies (Bio legend #100220). We used anti-mouse NK1.1 monoclonal mouse IgG2a antibodies (PK136) that can bind to all cells displaying FcR I, FcR II and/or FcR III. Since NK1.1 marker is lacking in C3H mice, these antibodies helped us quantify all splenic phagocytes. The cells were washed with PBS containing 5% FBS by centrifugation and resuspended in FACS buffer. BD LSRFortessa™ X-20 (BD Biosciences) driven by software FACS DiVa (BD Biosciences) was used for FACS data collection for the stained cells. Acquired data was analyzed using FlowJo, Version 10.3 software.

In vitro stimulation of transfected HEK293 cells.

The HEK293 cells were cultivated in 1:1 mixture of Dulbecco's Modified Eagle's Medium (DMEM) and Ham's F12 medium supplemented with 10% FBS and P/S mixture with G418 included for selection of transfection plasmids, i.e., pCDNA3 vector, plasmid containing TLR2-YFP fusion, TLR4-CFP fusion + flag tagged MD-2 in incubator set at 37°C and 5% CO_2. Confirmation of expression of respective TLRs by confocal microscopy was achieved by detecting fluorescence associated with respective fusion proteins. Heparinated *Bm* infected blood from C3H/HeJ mouse (30.7% parasitemia) was collected. After growing cells in 24 well plate (4 replicates), they were washed once with PBS and then added 500μl DMEM high glucose culture media with 10% FBS without any antibiotics, i.e., treatment medium (control), or the same medium containing $2x10^7$ N40 per well or $1x10^6$ RBCs (~$3.1x10^5$ iRBCs) per well per 500μl. In addition, *Bm* parasites were isolated by treatment of RBCs from infected mice with 0.15% saponin prepared in PBS by incubating on ice for 30 minutes followed by centrifugation at 2,000 xg to remove RBC debris. Released parasites pellet was obtained by centrifugation of supernatant at 10,000 xg for 10 minutes. The pellet was then suspended in treatment medium containing 20μg/ml Polymyxin B to eliminate the effect of LPS contamination, if any. Transfected 293 cell lines were also treated with N40 in Polymyxin B containing medium (not shown) or $1.25x10^7$ released *Bm* parasites suspension per well per 500μl. Plates were centrifuged in Beckman-Coulter Allegra-x14 bench top centrifuge at 900 xg and incubated overnight in 5% CO_2 incubator at 37°C for TLR stimulation. Supernatants were collected the next day (~16h incubation) and analyzed for cytokines secretion using ELISA kits from R & D Systems (Minneapolis, USA) following manufacturer's protocol. Experiment was conducted three times with 4 replicates for each treatment. Data from a representative experiment is presented here.

Statistical analysis.

All data collected were analyzed by GraphPad prism, version 7 for Windows (GraphPad Software, San Diego, California USA) and are presented as mean ± standard deviation (s.d.). Comparisons between two groups were made using unpaired, two-tailed Student t test with unequal variance, whereas ordinary one-way ANOVA assuming Gaussian distribution was used to determine significant difference between paired C3H/HeJ and C3H/HeN strain results. Values below 0.05 were considered significant for a paired group samples comparison at 95% confidence interval.

RESULTS

Bm parasitemia levels are not significantly affected by TLR4 functional attenuation in C3H mice.

To determine the effect of the dysfunctional TLR4 on infectivity, we monitored *Bm* parasitemia in C3H/HeJ and C3H/HeN mice infected singly or co-infected with *B. burgdorferi.* The onset of parasitemia appeared earlier in the C3H/HeN (7th day) than in C3H/HeJ mice (10th day) with net gain in *Bm* parasitemia. Due to similar kinetics of replication, peak parasitemia for C3H/HeN mice was on day 12 and for C3H/HeJ mice one day later, i.e., day 13, post-infection and the clearance of iRBCs by immune system was also slightly faster in C3H/HeN mice. In addition, parasitemia in C3H/HeJ mice, unlike C3H/HeN mice, remained detectable by microscopic examination until 20th day in *Bm*-infected mice as well as those co-infected with *B. burgdorferi* (Figure 1). The peak parasitemia levels between these two sets of mice were comparable when they were either infected by *Bm* alone (43.2±4.9% in HeJ versus 40.2±2.4% in HeN mice) or together with *B. burgdorferi* (36.0±3.7% in HeJ versus 33.5±5.3% in HeN mice); however, it is clear that peak parasitemia in both C3H/HeJ and C3H/HeN co-infected mice was significantly lower than that in respective *Bm* infected mouse strain. These results are reproducible. Even in the co-infected C3H/HeJ mice, parasitemia remains detectable by microscopic examination longer than in co-infected C3H/HeN mice. Similar pattern was also observed in *Bm* infected respective strains of mice (Figure 1).

Colonization of the head region, hearts, joints and skin by *B. burgdorferi* at 2 weeks of infection increases in the *Bm* co-infected respective mouse strains.

Our previous experiments have shown that peak *Bm* parasitemia and highest *B. burgdorferi* tissue colonization occur at two weeks of infection in the C3H/HeJ strain (V. Djokic, Akoolo, L., Primus, S., Schlachter, S., Kelly, K., Bhanot, P., and N. Parveen., 2019). To determine the impact of the inherent differences between C3H/HeN and C3H/HeJ strains on colonization of different organs by bioluminescent *B. burgdorferi* N40 strain in the presence or absence of co-infecting *Bm,* light emission was used as a measure of tissue colonization detected by live imaging of mice at two weeks of infection. We detected an overall higher colonization levels by N40 in mice co-infected with *Bm* as compared to those infected with *B. burgdorferi* alone in the respective mouse strains (Figure 2a and 2b). To further plot comparative levels of light emission in all *B. burgdorferi* infected mice, we determined total body bioluminescence radiance of infected (Figure 2a and 2b) and uninfected mice (Figure 2c). Net radiance in infected mice after deduction of average radiance from five

uninfected controls were calculated (Figure 2d). As apparent in the images shown (Figure 2a and 2b), total radiance was significantly higher in C3H/HeJ compared to C3H/HeN mice when infected only with N40 (Figure 2d, t=9.1, p<0.0001, 95% CI: 3982 – 6372). Difference in total radiance between co-infected C3H/HeJ and C3H/HeN mice was also significant with slightly higher radiance in C3H/HeJ mice; however, difference was not as pronounced as between respective N40-infected mice (t=3.1, p=0.006, 95% CI: 1308 – 6608). Difference between net bioluminescence in co-infected C3H/HeN mice compared to respective N40 infected strain was more pronounced (t=6.8, p<0.0001, 95% CI: 2894 – 5460) than difference observed in co-infected and N40-infected C3H/HeJ mice. This was because overall radiance was higher even in N40 infected C3H/HeJ group making its difference from co-infected mice not as high as observed in C3H/HeN mice (Figure 2d, t=2.4, p=0.03, 95% CI: 349 – 5567). In addition, co-infected C3H/HeN mice showed comparable bioluminescence radiance to N40-infected C3H/HeJ mice (t=0.2, p=0.81, 95% CI: −727 – 579).

Colonization of the specific organs by *B. burgdorferi* persists in singly infected, and *Bm* co-infected animals at 3 weeks of infection.

By three weeks of infection, the specific adaptive response develops against each pathogen and *Bm* parasitemia becomes undetectable microscopically (Figure 1). Difference in the light emission in joints and head of two strains of mice was higher in C3H/HeJ mice when infected with N40 alone (Figure 3a). Similarly, co-infected C3H/HeJ strain showed slightly higher colonization of joints as detected by bioluminescence (Figure 3b). In fact, net bioluminescence radiance, after deduction of average radiance obtained from five uninfected mice (Figure 3c), remained significantly higher in co-infected versus N40-infected C3H/HeJ (t=4.9, p=0.0001, 95% CI: 812–2044) and C3HHeN mice (t=4.8, p=0.0001, 95% CI: 705 – 1807); however, difference in average radiance between N40 infected C3H/HeJ and co-infected C3H/HeN animals was not statistically significant (Figure 3d). We also observed an overall decline in colonization by *B. burgdorferi* at three weeks compared to that at two weeks of respective infections in each strain of mice (Figures 2d and 3d). N40 survival and tissue colonization was further confirmed by recovering live spirochetes consistently when injection site, left ear and bladder from both strains of mice were recovered and grown in *B. burgdorferi* medium at three weeks post-infection (data not shown).

Higher *B. burgdorferi* burden in TLR4 depleted C3H/HeJ than in C3H/HeN mice at 3 weeks post-infection result in increased pathology.

After euthanasia at three weeks post-infection, we determined the effect of C3H/HeN and C3H/HeJ genotypes, in the context of functional TLR4 presence, on colonization of N40 when present alone, or with *Bm* in co-infected mice. The mice left hind legs (from hip to ankle), whole brain, and heart together with major vasculature (aorta and left vena cava) of mice were recovered and a duplex qPCR assay performed to quantify the spirochete levels normalized to mouse DNA content. The right hind legs including knee and tibiotarsus joints were used for histopathological examination. In mice infected with N40 alone, significantly higher spirochete loads were observed in the tissues of C3H/HeJ mice (dysfunctional TLR4) as compared to TLR4 competent C3H/HeN mice by qPCR (Figure 4a) confirming the results obtained by live imaging (Figure 3). In these mice, the burden of spirochetes in

each of three organs was ~2-fold higher in C3H/HeJ mice. In *Bm* and N40 co-infected mice, spirochetes burden was again higher in C3H/HeJ as compared to C3H/HeN mice in all three organs examined (Figure 4a), supporting our live imaging results (Figure 3). Co-infected mice had significantly higher numbers of spirochetes in brains and joints than singly infected mice irrespective of the mouse strain. The level of colonization of heart between N40 infected and co-infected mice was almost comparable in respective strains (Figure 4a, Not significant or $p < 0.05$). Burden of spirochetes was also higher in the hearts of both N40-infected and co-infected C3H/HeJ than in C3H/HeN mice.

We sought to evaluate if increased colonization by N40 during co-infection also enhanced pathology in mice possessing functional or non-functional TLR4. The joint sections were scored in a blinded manner to determine arthritis severity. Scoring of inflammation was based on infiltration of lymphocytes in the synovium and perisynovium, hyperplasia of the synovium, erosion or cellular infiltration of articular cartilage, increased synovial space (marked by arrows in the Figure 4b) etc. and severity of arthritis were ranked on a scale from (−), i.e., similar to uninfected mice, to (+++) for highly inflamed joints (Table 1). We observed inflammation of tibiotarsus in both *B. burgdorferi* infected C3H/HeJ and C3H/HeN mice (Figure 4b and Table 1) with a slight increase in pathology in C3H/HeJ mice reflecting the impact of higher burden of N40 in this mouse strain. More importantly, highest lymphocyte infiltration and hyperplasia of synovium was observed in co-infected C3H/HeJ mice compared to all other infected mice representing most pronounced inflammatory arthritis in these mice.

Modulation of splenic immune responses by infection with *Bm* and *B. burgdorferi* separately, or together at 3 weeks post-infection of C3H/HeJ and C3H/HeN mice.

To define the effect of functional TLR4 absence or presence in C3H/HeJ and C3H/HeN mice, respectively on the host immune response to *Bm* and *B. burgdorferi* infections, we studied the changes in different splenic myeloid and lymphoid cells of infected mice by quantification of total T cells (CD3+), natural killer (NK1.1+)/FcR+ cells, macrophages (F4/80+) and B (CD19+) cells. Changes in both myeloid and lymphoid splenic cells percentages in infected versus the naïve mice is shown (Figure 5). Since C3H mice lack the NK1.1 marker, it is likely that after B cells sorting by flow cytometry, NK1.1 label gated all phagocytic cells possessing FcR. A significant increase in macrophages was observed in all *Bm* infected and co-infected mice compared to N40 infected and naïve mice (Figure 5a). Interestingly, macrophage percentage increase in co-infected C3H/HeN strain was higher compared to both strains of mice infected with *B. burgdorferi* and *Bm* individually (Figure 5a). Total phagocytic (FcR+) cells increased significantly in all infected C3H/HeJ mice but only in N40 infected C3H/HeN mice (Figure 5b). Co-infected mice showed decreased in FcR+ cells in spleen as compared to N40 infected mice. We did not observe significant differences in percentages of macrophages between C3H/HeN and C3H/HeJ mice infected either with *B. burgdorferi* or *Bm* individually, while co-infection resulted in significant increases in percentages of macrophages in both strains of mice (Figure 5a). Thus, effect of infection with each pathogen is different on macrophage versus FcR+ phagocytic cells, both of which participate in innate immune response.

In both strains of mice infected with *B. burgdorferi* alone, we observed a significant increase in the percentages of total T cells; however, increase was higher in C3H/HeJ as compared to C3H/HeN mice (Figure 5c). The percentage of B cells increased significant only in N40 infected C3H/HeJ mice (Figure 5d). Changes in B and T cells in *Bm* infected, or co-infected mice were not significant relative to naïve mice (Figure 5c and 5d). All co-infected mice showed a significant decrease in the percentages of T and B cells as compared to *B. burgdorferi* infected and even *Bm* infected mice in most cases, particularly in TLR4 defective C3H/HeJ strain (Figure 5b, 5c and 5d). T cells percentages in co-infected mice were comparable in both mouse strains although their percentage diminished relative to *B. burgdorferi* infected mice (Figure 5c). Increases in FcR+ cells after *B. burgdorferi* infection were not as high in C3H/HeN mice as C3H/HeJ mice and decline in co-infected mice was also relatively lower in the former. No change in FcR+ and T cells percentage was detected in co-infected C3H/HeN mice as compared to naïve mice.

Signaling of TLR2/TLR4 transfected HEK293 cells with *B. burgdorferi* and *Bm* infected RBCs.

Enhanced response reported through TLR2 in the absence of TLR4 (Mu, Pennock, Humphreys, Kirschning, & Cole, 2005) suggests either increased expression and/or enhanced responsiveness of TLR2 to *B. burgdorferi* lipoproteins. Since such a response to Lyme spirochetes could be localized to the specific regions of organs, such as in the heart base and synovium of joints, quantification of each TLR by real-time PCR and their response to PAMPs in the particular regions is very difficult. Therefore, we decided to use a clean system of transfected cell line to evaluate signaling by PAMPs of *B. burgdorferi* and potentially *Bm*. Parental HEK293 cells do not express either TLR2 or TLR4. We used transfected HEK293 cells that stably express TLR2-YFP, or TLR4-CFP+Flag-tagged MD-2 and included control cells (pCDNA3 vector transfected) in our experiments that were generously provided by Dr. Golenbock (Latz et al., 2002). We confirmed the expression of respective TLRs by microscopy (Figure 6a and 6b). As compared to the medium treated HEK293 transfected cells (control), TLR2-transfected cells showed significant increase in production of IL-8 after stimulation by *B. burgdorferi* and caused induction of pro-inflammatory cytokines production even when 20μg/ml Polymyxin B was included in treatment medium (Figure 6d, 6h, and data not shown). Signaling of TLR4 by *B. burgdorferi* moderately increased IL-8 production; however, it was significantly higher than the control cell line treated with the same dose of spirochetes (Figure 6d and 6h). Neither TLR2 nor TLR4 signaling was observed in cells treated with *Bm* infected and diluted whole blood of mice that also possessed a few egressed parasites suggesting minimal levels or no *Bm* PAMPs were available for stimulation of these two TLRs (Figure 6e). Treatment of TLR transfected cell lines with 1.25×10^7 *Bm* parasites released by saponin treatment in the presence of Polymyxin B also did not show any stimulation (Figure 6f) indicating that either mature merozoites egressed from iRBCs are required for stimulation of TLRs on monocytes, macrophages, neutrophils, natural killer (NK) and dendritic cells during infection or *Bm* merozoites do not display PAMP on their surface for TLR signaling. A similar pattern was observed with respect to TNF-$_\alpha$ production by these cell line (Figure 6f to 6h) although levels of this cytokine were significantly lower than that observed for IL-8.

DISCUSSION

Transmission of *Bm* and *B. burgdorferi* occurs primarily through the bite of infected *Ixodes* species ticks. *Babesia* species were identified as infectious organisms in 1893 and babesiosis was first detected in humans in the U.S.A. in 1969 (Western et al., 1970; Ouhelli and Schein, 1988); however, delayed establishment of babesiosis in the endmeic regions for tick-borne diseases including Northeastern United States has been attributed to less efficient transmission of *Bm* by ticks compared to *B. burgdorferi* (Krause et al., 2006). Interestingly, acquisition of *Bm* from the white-footed mice by the tick vector improves when mice are co-infected with a highly infectious *B. burgdorferi* (Dunn et al., 2014). Diuk-Wasser et al. reported that incidence of babesiosis increases particularly in the regions where *B. burgdorferi* is already prevalent, thus suggesting that ongoing presence of *B. burgdorferi* in reservoir hosts and ticks promotes spread and establishment of *Bm* infection in the endemic regions (Diuk-Wasser et al., 2014). As a result, co-infections with these pathogens have started emerging in different regions of the World (Mayne, 2011, 2015, Anderson et al., 1991; Krause et al., 1991; Mitchell et al., 1996; Belongia, 2002, Swanson et al., 2006, Primus et al., 2018, Welc-Faleciak et al., 2010). This study was undertaken to better understand signaling of TLR2, in the presence or absence of functional TLR4, by PAMPs of both pathogens and resulting host immune responses in the absence of other mitigating factors. Therefore, a more controlled, needle-injection method with precise infection doses was used in our experiments. Although it does not reflect tick bite-mediated inoculation route, advantgae of this method is that it eliminates the effect of variability introduced during natural infection by ticks, which may not inoculate consistent dose of each pathogen in each set of inbred mice, thus making comparison rather difficult without using a large number of animals.

Despite evidence of high susceptibility of both TLR4 competent C3H/HeN mice and dysfunctional TLR4 possessing C3H/HeJ mice to *Bm* and *B. burgdorferi* infections, a comparative study of the pathogenesis of infections in these strains has not been conducted until now. We sought to examine the effect of TLR4 on *Bm* and *B. burgdorferi* when inoculated separately, or together. Although TLR4 ligand has not been identified in either *Bm* or *B. burgdorferi*; GPI glycolipid abundantly present in the membranes of many pathogenic protozoa has been identified as a possible TLR4 ligand (Debierre-Grockiego et al., 2007). We decided to address whether TLR4 is important for these tick-borne infections by assessing the differences in kinetics of growth patterns of *Bm* in blood, and burdens of *B. burgdorferi* in organs of the infected or co-infected C3H/HeJ and C3H/HeN mice. Overall, lower *Bm* peak parasitemia was observed in co-infected mice as compared to *Bm*-infected mice, but difference in peak parasitemia between two strains of C3H mice was not significant (Figure 1). Unlike the study by Coleman et al. (Coleman et al., 2005), we observed differences in *B. burgdorferi* colonization of different organs of co-infected C3H mice (Figures 1 to 4) that resulted in enhancement of Lyme disease pathology.

Both TLR4 and TLR2 activation has been shown to play critical roles in pathogenesis of arthritis (Abdollahi-Roodsaz et al., 2013; Campo et al., 2011). Abundant *B. burgdorferi* surface lipoproteins signal host cells primarily through TLR2 heterodimer and resulting in stimulation of proinflammatory cytokines production (Cervantes et al., 2011; Lien et al.,

1999; Salazar et al., 2009); however, other TLRs have also been implicated in disease and tolerance to infection (Cervantes et al., 2011; Cervantes et al., 2013; Gebbia, Coleman, & Benach, 2004; Hirschfeld et al., 1999; Salazar et al., 2005; Salazar et al., 2003; Shin et al., 2008). The role of TLR4 in control of the *B. burgdorferi* infections was based upon the observation that TLR4 defective bone marrow derived macrophages (BMDMs) from C3H/HeJ mice produced less TNF-α in response to *B. burgdorferi* infection, compared to BMDMs from normal TLR4 containing C3H/FeJ mice (Glickstein & Coburn, 2006). Consistent with the known requirement of TLR4 for full function of innate immune system, our results show a significant increase in overall N40 strain burden in C3H/HeJ mice at two weeks post-infection (Figure 2). Previously, *B. burgdorferi* infection in rhesus monkeys after TLR4 depletion, or after inhibition of its functional activity showed opposite effect on inflammatory responses in the neuronal tissues (Parthasarathy & Philipp, 2015). Control of *B. burgdorferi* infection was found to be dependent upon phagocytosis mediated killing through spirochete lipoproteins signaling after recognition of TLR2 (Hirschfeld et al., 1999), while higher proinflammatory cytokine production could attenuate *B. burgdorferi* infection in TLR4 sufficient mice by a still unknown PAMP (Glickstein & Coburn, 2006). Signaling through mainly TLR2, and to a lesser extent TLR4 by *B. burgdorferi* to produce proinflammatory cytokines was confirmed by our *in vitro* experiments using the specific TLR-transfected HEK 293 cells (Figure 6). The absence of functional TLR4 in C3H/HeJ mice could be responsible for preventing early bacterial clearance and lead to increased tissue invasion by *B. burgdorferi* compared to that in C3H/HeN mice while spirochetes burden in various organs becomes almost comparable at three weeks post-infection after adaptive immune response was established (Figures 2 and 3).

Higher burden of spirochetes was previously reported to also reflect more severe arthritis in infected patients and a similar pattern was also observed in mice (Diuk-Wasser et al., 2016; Krause et al., 1996; Moro et al., 2002). Indeed, we observed higher pathology in C3H/HeJ than C3H/HeN mice when co-infected with *Bm* (Figure 4). Although genotype-based resistance of some mouse strains to Lyme arthritis irrespective of *B. burgdorferi* quantities in joints had been observed (Bramwell et al., 2014; C. R. Brown & Reiner, 1999; Pahl, Kuhlbrandt, Brune, Rollinghoff, & Gessner, 1999; Wooten & Weis, 2001), N40 burden correlated with the severity of Lyme arthritis within the same strain of mice in our study. *Bm* infection of mice activates CD4+ T cells and results in production of IFN-γ that could further activate macrophages leading to Th1 response stimulation (Igarashi et al., 1999). In our recent studies in young C3H/HeJ mice, Th1 cells proliferation and response demonstrated by intracellular IFN-γ production was most pronounced during early acute stage of infection (before peak parasitemia, on day 11) with *Bm.* These results indicated that Th1 cells likely play an important role in resolution of parasitemia (V. Djokic et al., 2018). A significant increase in Th1 cells in N40 infected and co-infected mice at this time point suggested that these CD4+ cells likely contributed to the clearance of both pathogens during acute phase of infection. There was no significant change in CD19+ B cells in infected C3H/HeJ mice at the early phase of infection in that study (V. Djokic et al., 2018).

In our previous study, we observed a significant increase in myeloid cell numbers in C3H/HeJ infected mice at acute phase with total macrophage numbers increased in both *Bm* infected, and N40 co-infected mice relatively more than in N40 infected mice (V.

Djokic et al., 2018). The activation of macrophages also results in TNF-$_\alpha$, reactive oxygen species and nitric oxide production (Homer et al., 2000), which together enhance their microbicidal activity. A significant proliferation of FcR+, representing primarily phagocytic cells in infected C3H/HeJ mice suggests that these cells may also be involved in clearance of both *B. burgdorferi* and *Bm* at the acute phase of infection. Although C3H/HeJ macrophages fail to induce inflammatory cytokines in response to microbial TLR4 stimulants like LPS (Hoshino et al., 1999), the role of PAMPS of *Bm* in TLR-NF-k$_\beta$ activation pathway to cause macrophages activation soon after infection is not known. The absence of detectable differences in *Bm* parasitemia development and resolution in *Bm* infected C3H/HeJ and C3H/HeN mice alone, or with *B. burgdorferi*, suggests that TLR2 and TLR4 signaling do not contribute significantly to *Bm* clearance. Our results agree with previous study by Skariah and coworkers, who showed that MyD88 deficiency did not affect *Bm* parasitemia in mice (Skariah et al., 2017). Furthermore, the lack of stimulation of TLR2 and TLR4 in transfected HEK293 cells to the whole blood from *Bm*-infected C3H mice, which contained iRBCs as well as egressed parasites that should display GPI-anchored proteins on their surface such as BmGPI12 (Thekkiniath et al., 2019; Thekkiniath et al., 2018), in our *in vitro* experiment confirmed the lack of response of these PRRs to *Bm* (Figure 6). These results also confirmed our *in vivo* data.

Previous studies have shown enhanced activity of TLR2 in the hosts deficient in TLR4 (Mu et al., 2005). It is therefore expected that the activity of TLR2 in C3H/HeJ mice could also be higher during *B. burgdorferi* infection due to the absence of TLR4, thus increasing inflammation in this mouse strain. TLRs form a crucial link between innate and adaptive immunity by up-regulating the ability of accessory cells to generate immune responses mediated by T and B lymphocytes (Iwasaki & Medzhitov, 2010). In fact, we observed significantly higher levels of B and T cells in C3H/HeJ strain at three weeks of infection with *B. burgdorferi* that greatly diminished in the presence of *Bm* (Figure 5). Slight delay in resolution of *Bm* infection in TLR4-defective mice can be attributed to their somewhat attenuated adaptive immune response.

To summarize, our results demonstrate that TLR4 may also play an indirect role in modulating immune response and pathology during *B. burgdorferi* infections. We propose that activation of TLR4 by unknown ligands from co-infecting pathogens in C3H/HeN mice, more importantly from *B. burgdorferi*, could down regulate TLR2 heterodimeric receptor, as described previously (Mu et al., 2005), particularly in peripheral blood nucleated cells early in infection, thus reducing signaling through MyD88 dependent (or independent) pathway which then suppresses inflammatory immune responses (Figures 4 to 6). In the absence of functional TLR4 in C3H/HeJ mice, unrestrained stimulation could occur through TLR2 signaling due to the abundance of lipoproteins on spirochetes surface, causing more pronounced inflammatory response in *B. burgdorferi* infected and co-infected C3H/HeJ mice as compared to C3H/HeN mice (graphical abstract). The effect of *Bm* PAMPS on TLR2/TLR4 signaling-mediated innate immune response in both strains of mice during infection, whether present alone or with *B. burgdorferi,* appears minimal (Figure 1). These results were further confirmed using transfected HEK293 cell lines *in vitro* (Figure 6) suggesting the absence of display of *Bm* PAMPs, such as GPI anchored proteins, on iRBCs surface.

DATA AVAILABILITY STATEMENT

All data are fully available without restriction.

ABBREVIATIONS

TLR	Toll Like Receptor
qPCR	Real-time quantitative polymerase chain reaction
PAMP	Pathogen associated molecular patterns
PRRs	pattern recognition receptors
RBCs	Red blood cells
NK	Natural killer
GPI	glycosylphosphatidylinositol
IACUC	Institutional Animal Care and Use Committee
SCID	severe combined immunodeficient
ACK	Ammonium-Chloride–Potassium
BSKII	Barbour-Stoenner-Kelly-II
RS	Rabbit serum
IVIS	In Vivo Imaging System
s.c.	subcutaneous
i.p.	intraperitoneal

REFERENCES

Abdollahi-Roodsaz S, Koenders MI, Walgreen B, Bolscher J, Helsen MM, van den Bersselaar LA, … van den Berg WB (2013). Toll-like receptor 2 controls acute immune complex-driven arthritis in mice by regulating the inhibitory Fcgamma receptor IIB. Arthritis Rheum, 65(10), 2583–2593. doi:10.1002/art.38087 [PubMed: 23860661]

Aliota MT, Dupuis AP 2nd, Wilczek MP, Peters RJ, Ostfeld RS, & Kramer LD (2014). The prevalence of zoonotic tick-borne pathogens in Ixodes scapularis collected in the Hudson Valley,

New York State. Vector Borne Zoonotic Dis, 14(4), 245–250. doi:10.1089/vbz.2013.1475 [PubMed: 24689680]

Armstrong AL, Barthold SW, Persing DH, & Beck DS (1992). Carditis in Lyme disease susceptible and resistant strains of laboratory mice infected with *Borrelia burgdorferi*. Am J Trop Med Hyg, 47(2), 249–258. [PubMed: 1503192]

Baravalle ME, Thompson C, de Echaide ST, Palacios C, Valentini B, Suarez CE, … Echaide I (2010). The novel protein BboRhop68 is expressed by intraerythrocytic stages of *Babesia bovis*. Parasitol Int, 59(4), 571–578. doi:10.1016/j.parint.2010.07.008 [PubMed: 20691808]

Barthold SW (1991). Infectivity of *Borrelia burgdorferi* relative to route of inoculation and genotype in laboratory mice. J Infect Dis, 163, 419–420. [PubMed: 1988530]

Barthold SW, Beck DS, Hansen GM, Terwilliger GA, & Moody KD (1990). Lyme borreliosis in selected strains and ages of laboratory mice. J Infect Dis, 162(1), 133–138. [PubMed: 2141344]

Benoit VM, Petrich A, Alugupalli KR, Marty-Roix R, Moter A, Leong JM, & Boyartchuk VL (2010). Genetic control of the innate immune response to *Borrelia hermsii* influences the course of relapsing fever in inbred strains of mice. Infect Immun, 78(2), 586–594. doi:10.1128/IAI.01216-09 [PubMed: 19995898]

Borggraefe I, Yuan J, Telford SR 3rd, Menon S, Hunter R, Shah S, … Vannier E (2006). *Babesia microti* primarily invades mature erythrocytes in mice. Infect Immun, 74(6), 3204–3212. doi:10.1128/IAI.01560-05 [PubMed: 16714547]

Bose R (1994). Polyclonal antibody characterization of *Babesia caballi* antigens. Int J Parasitol, 24(4), 511–517. [PubMed: 7521861]

Bramwell KK, Ma Y, Weis JH, Chen X, Zachary JF, Teuscher C, & Weis JJ (2014). Lysosomal beta-glucuronidase regulates Lyme and rheumatoid arthritis severity. The Journal of clinical investigation, 124(1), 311–320. doi:10.1172/JCI72339 [PubMed: 24334460]

Brown CR, & Reiner SL (1999). Genetic control of experimental lyme arthritis in the absence of specific immunity. Infect Immun, 67(4), 1967–1973. [PubMed: 10085044]

Brown WC, Norimine J, Knowles DP, & Goff WL (2006). Immune control of Babesia bovis infection. Vet Parasitol, 138(1–2), 75–87. doi:10.1016/j.vetpar.2006.01.041 [PubMed: 16510249]

Bulut Y, Faure E, Thomas L, Equils O, & Arditi M (2001). Cooperation of Toll-like receptor 2 and 6 for cellular activation by soluble tuberculosis factor and *Borrelia burgdorferi* outer surface protein A lipoprotein: role of Toll-interacting protein and IL-1 receptor signaling molecules in Toll-like receptor 2 signaling. J Immunol, 167(2), 987–994. [PubMed: 11441107]

Campo GM, Avenoso A, Nastasi G, Micali A, Prestipino V, Vaccaro M, … Campo S (2011). Hyaluronan reduces inflammation in experimental arthritis by modulating TLR-2 and TLR-4 cartilage expression. Biochim Biophys Acta, 1812(9), 1170–1181. doi:10.1016/j.bbadis.2011.06.006 [PubMed: 21723389]

Campos MA, Almeida IC, Takeuchi O, Akira S, Valente EP, Procopio DO, … Gazzinelli RT (2001). Activation of Toll-like receptor-2 by glycosylphosphatidylinositol anchors from a protozoan parasite. J Immunol, 167(1), 416–423. doi:10.4049/jimmunol.167.1.416 [PubMed: 11418678]

Caulfield AJ, & Pritt BS (2015). Lyme Disease Coinfections in the United States. Clin Lab Med, 35(4), 827–846. doi:10.1016/j.cll.2015.07.006 [PubMed: 26593260]

Cervantes JL, Dunham-Ems SM, La Vake CJ, Petzke MM, Sahay B, Sellati TJ, … Salazar JC (2011). Phagosomal signaling by Borrelia burgdorferi in human monocytes involves Toll-like receptor (TLR) 2 and TLR8 cooperativity and TLR8-mediated induction of IFN-beta. Proc Natl Acad Sci U S A, 108(9), 3683–3688. doi:10.1073/pnas.1013776108 [PubMed: 21321205]

Cervantes JL, La Vake CJ, Weinerman B, Luu S, O'Connell C, Verardi PH, & Salazar JC (2013). Human TLR8 is activated upon recognition of *Borrelia burgdorferi* RNA in the phagosome of human monocytes. J Leukoc Biol, 94(6), 1231–1241. doi:10.1189/jlb.0413206 [PubMed: 23906644]

Chan K, Alter L, Barthold SW, and Parveen N (2015). Disruption of bbe02 by insertion of a luciferase gene increases transformation efficiency of Borrelia burgdorferi and allows live imaging in Lyme disease susceptible C3H mice PLoS One, 10(6) (e0129532). doi:10.1371/journal.pone.0129532 [PubMed: 26069970]

Chan K, Marras SA, & Parveen N (2013). Sensitive multiplex PCR assay to differentiate Lyme spirochetes and emerging pathogens *Anaplasma phagocytophilum* and *Babesia microti*. BMC microbiology, 13, 295. doi:10.1186/1471-2180-13-295 [PubMed: 24359556]

Chow JC, Young DW, Golenbock DT, Christ WJ, & Gusovsky F (1999). Toll-like receptor-4 mediates lipopolysaccharide-induced signal transduction. Journal of Biological Chemistry, 274(16), 10689–10692. doi:DOI 10.1074/jbc.274.16.10689

Coleman JL, LeVine D, Thill C, Kuhlow C, & Benach JL (2005). *Babesia microti* and *Borrelia burgdorferi* follow independent courses of infection in mice. J Infect Dis, 192(9), 1634–1641. doi:10.1086/496891 [PubMed: 16206079]

Debierre-Grockiego F, Campos MA, Azzouz N, Schmidt J, Bieker U, Resende MG, … Schwarz RT (2007). Activation of TLR2 and TLR4 by glycosylphosphatidylinositols derived from *Toxoplasma gondii*. J Immunol, 179(2), 1129–1137. doi:10.4049/jimmunol.179.2.1129 [PubMed: 17617606]

Debierre-Grockiego F, Smith TK, Delbecq S, Ducournau C, Lantier L, Schmidt J, … Cornillot E (2019). *Babesia divergens* glycosylphosphatidylinositols modulate blood coagulation and induce Th2-biased cytokine profiles in antigen presenting cells. Biochimie, 167, 135–144. doi:10.1016/j.biochi.2019.09.007 [PubMed: 31585151]

Delbecq S, Precigout E, Vallet A, Carcy B, Schetters TP, & Gorenflot A (2002). *Babesia divergens*: cloning and biochemical characterization of Bd37. Parasitology, 125(Pt 4), 305–312. doi:10.1017/s0031182002002160 [PubMed: 12403318]

Diuk-Wasser MA, Vannier E, & Krause PJ (2016). Coinfection by *Ixodes* Tick-Borne Pathogens: Ecological, Epidemiological, and Clinical Consequences. Trends Parasitol, 32(1), 30–42. doi:10.1016/j.pt.2015.09.008 [PubMed: 26613664]

Djokic V, Akoolo L, Primus S, Schlachter S, Kelly K, Bhanot P, and Parveen N. (2019). Protozoan parasite *Babesia microti* subverts adaptive immunity and enhances Lyme disease severity. Froniters in Microbiology, 10, 1596. doi:doi: 10.3389/fmicb.2019.01596

Djokic V AL, Parveen N (2018). *Babesia microti* Infection Changes Host Spleen Architecture and Is Cleared by a Th1 Immune Response. Froniters in Microbiology, 9, 1–11. doi:doi: 10.3389/fmicb.2018.00085

Djokic V, Primus S, Akoolo L, Chakraborti M, & Parveen N (2018). Age-Related Differential Stimulation of Immune Response by *Babesia microti* and *Borrelia burgdorferi* During Acute Phase of Infection Affects Disease Severity. Front Immunol, 9, 2891. doi:10.3389/fimmu.2018.02891 [PubMed: 30619263]

Dunn JM, Krause PJ, Davis S, Vannier EG, Fitzpatrick MC, Rollend L, … Diuk-Wasser MA (2014). *Borrelia burgdorferi* promotes the establishment of *Babesia microti* in the northeastern United States. PLoS One, 9(12), e115494. doi:10.1371/journal.pone.0115494 [PubMed: 25545393]

Fallahi P, Elia G, & Bonatti A (2017). Interferon-gamma-induced protein 10 in Lyme disease. Clin Ter, 168(2), e146–e150. doi:10.7417/CT.2017.1997 [PubMed: 28383628]

Gautam A, Dixit S, Embers M, Gautam R, Philipp MT, Singh SR, … Dennis VA (2012). Different patterns of expression and of IL-10 modulation of inflammatory mediators from macrophages of Lyme disease-resistant and -susceptible mice. PLoS One, 7(9), e43860. doi:10.1371/journal.pone.0043860 [PubMed: 23024745]

Gebbia JA, Coleman JL, & Benach JL (2004). Selective induction of matrix metalloproteinases by *Borrelia burgdorferi* via toll-like receptor 2 in monocytes. J Infect Dis, 189(1), 113–119. [PubMed: 14702161]

Glickstein LJ, & Coburn JL (2006). Short report: Association of macrophage inflammatory response and cell death after in vitro Borrelia burgdorferi infection with arthritis resistance. Am J Trop Med Hyg, 75(5), 964–967. [PubMed: 17123997]

Gowda DC (2007). TLR-mediated cell signaling by malaria GPIs. Trends Parasitol, 23(12), 596–604. doi:10.1016/j.pt.2007.09.003 [PubMed: 17980663]

Gronberg-Hernandez J, Sunden F, Connolly J, Svanborg C, & Wullt B (2011). Genetic control of the variable innate immune response to asymptomatic bacteriuria. PLoS One, 6(11), e28289. doi:10.1371/journal.pone.0028289 [PubMed: 22140570]

Hagberg L, Briles DE, & Eden CS (1985). Evidence for separate genetic defects in C3H/HeJ and C3HeB/FeJ mice, that affect susceptibility to gram-negative infections. J Immunol, 134(6), 4118–4122. [PubMed: 3886795]

Hagberg L, Hull R, Hull S, McGhee JR, Michalek SM, & Svanborg Eden C (1984). Difference in susceptibility to gram-negative urinary tract infection between C3H/HeJ and C3H/HeN mice. Infect Immun, 46(3), 839–844. [PubMed: 6389367]

Heine H, & Lien E (2003). Toll-like receptors and their function in innate and adaptive immunity. Int Arch Allergy Immunol, 130(3), 180–192. doi:10.1159/000069517 [PubMed: 12660422]

Hersh MH, Ostfeld RS, McHenry DJ, Tibbetts M, Brunner JL, Killilea ME, … Keesing F (2014). Co-infection of blacklegged ticks with *Babesia microti* and *Borrelia burgdorferi* is higher than expected and acquired from small mammal hosts. PLoS One, 9(6), e99348. doi:10.1371/journal.pone.0099348 [PubMed: 24940999]

Herwaldt BL, Linden JV, Bosserman E, Young C, Olkowska D, & Wilson M (2011). Transfusion-associated babesiosis in the United States: a description of cases. Annals of Internal Medicine, 155(8), 509–519. doi:10.1059/0003-4819-155-8-201110180-00362 [PubMed: 21893613]

Hirschfeld M, Kirschning CJ, Schwandner R, Wesche H, Weis JH, Wooten RM, & Weis JJ (1999). Cutting edge: inflammatory signaling by *Borrelia burgdorferi* lipoproteins is mediated by toll-like receptor 2. J Immunol, 163(5), 2382–2386. [PubMed: 10452971]

Homer MJ, Aguilar-Delfin I, Telford SR 3rd, Krause PJ, & Persing DH (2000). Babesiosis. Clin Microbiol Rev, 13(3), 451–469. [PubMed: 10885987]

Horowitz HW, Aguero-Rosenfeld ME, Holmgren D, McKenna D, Schwartz I, Cox ME, & Wormser GP (2013). Lyme disease and human granulocytic anaplasmosis coinfection: impact of case definition on coinfection rates and illness severity. Clinical infectious diseases : an official publication of the Infectious Diseases Society of America, 56(1), 93–99. doi:10.1093/cid/cis852 [PubMed: 23042964]

Hoshino K, Takeuchi O, Kawai T, Sanjo H, Ogawa T, Takeda Y, … Akira S (1999). Cutting edge: Toll-like receptor 4 (TLR4)-deficient mice are hyporesponsive to lipopolysaccharide: evidence for TLR4 as the Lps gene product. J Immunol, 162(7), 3749–3752. [PubMed: 10201887]

Igarashi I, Suzuki R, Waki S, Tagawa Y, Seng S, Tum S, … Toyoda Y (1999). Roles of CD4(+) T cells and gamma interferon in protective immunity against Babesia microti infection in mice. Infect Immun, 67(8), 4143–4148. [PubMed: 10417185]

Iwasaki A, & Medzhitov R (2010). Regulation of Adaptive Immunity by the Innate Immune System. Science, 327(5963), 291–295. doi:10.1126/science.1183021 [PubMed: 20075244]

Jahfari S, Hofhuis A, Fonville M, van der Giessen J, van Pelt W, & Sprong H (2016). Molecular Detection of Tick-Borne Pathogens in Humans with Tick Bites and Erythema Migrans, in the Netherlands. PLoS Negl Trop Dis, 10(10), e0005042. doi:10.1371/journal.pntd.0005042 [PubMed: 27706159]

Knapp KL, & Rice NA (2015). Human Coinfection with *Borrelia burgdorferi* and *Babesia microti* in the United States. J Parasitol Res, 2015, 587131. doi:10.1155/2015/587131 [PubMed: 26697208]

Krause PJ, Gewurz BE, Hill D, Marty FM, Vannier E, Foppa IM, … Spielman A (2008). Persistent and relapsing babesiosis in immunocompromised patients. Clin Infect Dis, 46(3), 370–376. doi:10.1086/525852 [PubMed: 18181735]

Krause PJ, McKay K, Gadbaw J, Christianson D, Closter L, Lepore T, … Spielman A (2003). Increasing health burden of human babesiosis in endemic sites. The American journal of tropical medicine and hygiene, 68(4), 431–436. [PubMed: 12875292]

Krause PJ, McKay K, Thompson CA, Sikand VK, Lentz R, Lepore T, … Deer-Associated Infection Study, G. (2002). Disease-specific diagnosis of coinfecting tickborne zoonoses: babesiosis, human granulocytic ehrlichiosis, and Lyme disease. Clin Infect Dis, 34(9), 1184–1191. doi:10.1086/339813 [PubMed: 11941544]

Krause PJ, Spielman A, Telford SR 3rd, Sikand VK, McKay K, Christianson D, … Persing DH (1998). Persistent parasitemia after acute babesiosis. N Engl J Med, 339(3), 160–165. doi:10.1056/NEJM199807163390304 [PubMed: 9664092]

Krause PJ, Telford SR 3rd, Spielman A, Sikand V, Ryan R, Christianson D, … Persing DH (1996). Concurrent Lyme disease and babesiosis. Evidence for increased severity and duration of illness. JAMA, 275(21), 1657–1660. [PubMed: 8637139]

Kugeler KJ, Schwartz AM, Delorey MJ, Mead PS, & Hinckley AF (2021). Estimating the Frequency of Lyme Disease Diagnoses, United States, 2010–2018. Emerg Infect Dis, 27(2), 616–619. doi:10.3201/eid2702.202731 [PubMed: 33496229]

Lasky CE, Pratt CL, Hilliard KA, Jones JL, & Brown CR (2016). T Cells Exacerbate Lyme Borreliosis in TLR2-Deficient Mice. Front Immunol, 7, 468. doi:10.3389/fimmu.2016.00468 [PubMed: 27857714]

Latz E, Visintin A, Lien E, Fitzgerald KA, Monks BG, Kurt-Jones EA, … Espevik T (2002). Lipopolysaccharide rapidly traffics to and from the Golgi apparatus with the toll-like receptor 4-MD-2-CD14 complex in a process that is distinct from the initiation of signal transduction. J Biol Chem, 277(49), 47834–47843. [PubMed: 12324469]

Lien E, Sellati TJ, Yoshimura A, Flo TH, Rawadi G, Finberg RW, … Golenbock DT (1999). Toll-like receptor 2 functions as a pattern recognition receptor for diverse bacterial products. J Biol Chem, 274(47), 33419–33425. [PubMed: 10559223]

Liu N, Montgomery RR, Barthold SW, & Bockenstedt LK (2004). Myeloid differentiation antigen 88 deficiency impairs pathogen clearance but does not alter inflammation in *Borrelia burgdorferi*-infected mice. Infect Immun, 72(6), 3195–3203. [PubMed: 15155621]

Lommano E, Bertaiola L, Dupasquier C, & Gern L (2012). Infections and coinfections of questing *Ixodes ricinus* ticks by emerging zoonotic pathogens in Western Switzerland. Applied and environmental microbiology, 78(13), 4606–4612. doi:10.1128/AEM.07961-11 [PubMed: 22522688]

Lorenz E, Mira JP, Cornish KL, Arbour NC, & Schwartz DA (2000). A novel polymorphism in the toll-like receptor 2 gene and its potential association with staphylococcal infection. Infect Immun, 68(11), 6398–6401. [PubMed: 11035751]

Love AC, Schwartz I, & Petzke MM (2014). Borrelia burgdorferi RNA induces type I and III interferons via Toll-like receptor 7 and contributes to production of NF-kappaB-dependent cytokines. Infect Immun, 82(6), 2405–2416. doi:10.1128/IAI.01617-14 [PubMed: 24664510]

Mockenhaupt FP, Cramer JP, Hamann L, Stegemann MS, Eckert J, Oh NR, … Schumann RR (2006a). Toll-like receptor (TLR) polymorphisms in African children: Common TLR-4 variants predispose to severe malaria. Proc Natl Acad Sci U S A, 103(1), 177–182. doi:10.1073/pnas.0506803102 [PubMed: 16371473]

Mockenhaupt FP, Cramer JP, Hamann L, Stegemann MS, Eckert J, Oh NR, … Schumann RR (2006b). Toll-like receptor (TLR) polymorphisms in African children: common TLR-4 variants predispose to severe malaria. J Commun Dis, 38(3), 230–245. [PubMed: 17373355]

Moro MH, Zegarra-Moro OL, Bjornsson J, Hofmeister EK, Bruinsma E, Germer JJ, & Persing DH (2002). Increased arthritis severity in mice coinfected with *Borrelia burgdorferi* and *Babesia microti*. J Infect Dis, 186(3), 428–431. doi:10.1086/341452 [PubMed: 12134242]

Morr M, Takeuchi O, Akira S, Simon MM, & Muhlradt PF (2002). Differential recognition of structural details of bacterial lipopeptides by toll-like receptors. Eur J Immunol, 32(12), 3337–3347. doi:10.1002/1521-4141(200212)32:12<3337::AID-IMMU3337>3.0.CO;2-# [PubMed: 12432564]

Moutailler S, Valiente Moro C, Vaumourin E, Michelet L, Tran FH, Devillers E, … Vayssier-Taussat M (2016). Co-infection of Ticks: The Rule Rather Than the Exception. PLoS Negl Trop Dis, 10(3), e0004539. doi:10.1371/journal.pntd.0004539 [PubMed: 26986203]

Mu HH, Pennock ND, Humphreys J, Kirschning CJ, & Cole BC (2005). Engagement of Toll-like receptors by mycoplasmal superantigen: downregulation of TLR2 by MAM/TLR4 interaction. Cellular Microbiology, 7(6), 789–797. doi:10.1111/j.1462-5822.2005.00511.x [PubMed: 15888082]

Nagai Y, Akashi S, Nagafuku M, Ogata M, Iwakura Y, Akira S, … Miyake K (2002). Essential role of MD-2 in LPS responsiveness and TLR4 distribution. Nat Immunol, 3(7), 667–672. doi:10.1038/ni809 [PubMed: 12055629]

Nathaly Wieser S, Schnittger L, Florin-Christensen M, Delbecq S, & Schetters T (2019). Vaccination against babesiosis using recombinant GPI-anchored proteins. Int J Parasitol, 49(2), 175–181. doi:10.1016/j.ijpara.2018.12.002 [PubMed: 30684517]

Oosting M, Berende A, Sturm P, Ter Hofstede HJ, de Jong DJ, Kanneganti TD, … Joosten LA (2010). Recognition of *Borrelia burgdorferi* by NOD2 is central for the induction of an inflammatory reaction. J Infect Dis, 201(12), 1849–1858. doi:10.1086/652871 [PubMed: 20441518]

Pahl A, Kuhlbrandt U, Brune K, Rollinghoff M, & Gessner A (1999). Quantitative detection of *Borrelia burgdorferi* by real-time PCR. J Clin Microbiol, 37(6), 1958–1963. [PubMed: 10325354]

Panczuk A, Tokarska-Rodak M, Koziol-Montewka M, & Plewik D (2016). The incidence of B*orrelia burgdorferi, Anaplasma phagocytophilum* and *Babesia microti* coinfections among foresters and farmers in eastern Poland. J Vector Borne Dis, 53(4), 348–354. [PubMed: 28035112]

Parthasarathy G, & Philipp MT (2015). Inflammatory mediator release from primary rhesus microglia in response to *Borrelia burgdorferi* results from the activation of several receptors and pathways. J Neuroinflammation, 12, 60. doi:10.1186/s12974-015-0274-z [PubMed: 25889406]

Piesman J, Mather TN, Donahue JG, Levine J, Campbell JD, Karakashian SJ, & Spielman A (1986). Comparative prevalence of *Babesia microti* and *Borrelia burgdorferi* in four populations of *Ixodes dammini* in eastern Massachusetts. Acta Trop, 43(3), 263–270. [PubMed: 2430433]

Primus S, Akoolo L, Schlachter S, Gedroic K, Rojtman AD, & Parveen N (2018). Efficient detection of symptomatic and asymptomatic patient samples for *Babesia microti* and *Borrelia burgdorferi* infection by multiplex qPCR. PLoS One, 13(5), e0196748. doi:10.1371/journal.pone.0196748 [PubMed: 29746483]

Rahman S, Shering M, Ogden NH, Lindsay R, & Badawi A (2016). Toll-like receptor cascade and gene polymorphism in host-pathogen interaction in Lyme disease. J Inflamm Res, 9, 91–102. doi:10.2147/JIR.S104790 [PubMed: 27330321]

Rizzoli A, Silaghi C, Obiegala A, Rudolf I, Hubalek Z, Foldvari G, … Kazimirova M (2014). Ixodes ricinus and Its Transmitted Pathogens in Urban and Peri-Urban Areas in Europe: New Hazards and Relevance for Public Health. Front Public Health, 2, 251. doi:10.3389/fpubh.2014.00251 [PubMed: 25520947]

Rupprecht TA, Kirschning CJ, Popp B, Kastenbauer S, Fingerle V, Pfister HW, & Koedel U (2007). Borrelia garinii induces CXCL13 production in human monocytes through Toll-like receptor 2. Infect Immun, 75(9), 4351–4356. doi:10.1128/IAI.01642-06 [PubMed: 17562761]

Salazar JC, Duhnam-Ems S, La Vake C, Cruz AR, Moore MW, Caimano MJ, … Radolf JD (2009). Activation of human monocytes by live *Borrelia burgdorferi* generates TLR2-dependent and -independent responses which include induction of IFN-beta. PLoS Pathog, 5(5), e1000444. doi:10.1371/journal.ppat.1000444 [PubMed: 19461888]

Salazar JC, Pope CD, Moore MW, Pope J, Kiely TG, & Radolf JD (2005). Lipoprotein-dependent and -independent immune responses to spirochetal infection. Clin Diagn Lab Immunol, 12(8), 949–958. [PubMed: 16085913]

Salazar JC, Pope CD, Sellati TJ, Feder HM Jr., Kiely TG, Dardick KR, … Lyme Disease N (2003). Coevolution of markers of innate and adaptive immunity in skin and peripheral blood of patients with erythema migrans. J Immunol, 171(5), 2660–2670. [PubMed: 12928420]

Schlachter S, Chan K, Marras SAE, & Parveen N (2017). Detection and Differentiation of Lyme Spirochetes and Other Tick-Borne Pathogens from Blood Using Real-Time PCR with Molecular Beacons. Methods Mol Biol, 1616, 155–170. doi:10.1007/978-1-4939-7037-7_10 [PubMed: 28600768]

Schromm AB, Lien E, Henneke P, Chow JC, Yoshimura A, Heine H, … Golenbock DT (2001). Molecular genetic analysis of an endotoxin nonresponder mutant cell line: a point mutation in a conserved region of MD-2 abolishes endotoxin-induced signaling. J Exp Med, 194(1), 79–88. doi:10.1084/jem.194.1.79 [PubMed: 11435474]

Schulze TL, Jordan RA, Healy SP, & Roegner VE (2013). Detection of Babesia microti and Borrelia burgdorferi in host-seeking Ixodes scapularis (Acari: Ixodidae) in Monmouth County, New Jersey. J Med Entomol, 50(2), 379–383. [PubMed: 23540127]

Seixas E, Moura Nunes JF, Matos I, & Coutinho A (2009). The interaction between DC and *Plasmodium berghei/chabaudi*-infected erythrocytes in mice involves direct cell-to-cell contact,

internalization and TLR. Eur J Immunol, 39(7), 1850–1863. doi:10.1002/eji.200838403 [PubMed: 19585512]

Shimazu R, Akashi S, Ogata H, Nagai Y, Fukudome K, Miyake K, & Kimoto M (1999). MD-2, a molecule that confers lipopolysaccharide responsiveness on Toll-like receptor 4. J Exp Med, 189(11), 1777–1782. doi:10.1084/jem.189.11.1777 [PubMed: 10359581]

Shin OS, Isberg RR, Akira S, Uematsu S, Behera AK, & Hu LT (2008). Distinct roles for MyD88 and Toll-like receptors 2, 5, and 9 in phagocytosis of Borrelia burgdorferi and cytokine induction. Infect Immun, 76(6), 2341–2351. doi:10.1128/IAI.01600-07 [PubMed: 18378636]

Skariah S, Arnaboldi P, Dattwyler RJ, Sultan AA, Gaylets C, Walwyn O, … Mordue DG (2017). Elimination of Babesia microti Is Dependent on Intraerythrocytic Killing and CD4+ T Cells. J Immunol, 199(2), 633–642. doi:10.4049/jimmunol.1601193 [PubMed: 28607116]

Steere AC (2001). Lyme disease. N Engl J Med, 345(2), 115–125. [PubMed: 11450660]

Suarez CE, Laughery JM, Bastos RG, Johnson WC, Norimine J, Asenzo G, … Goff WL (2011). A novel neutralization sensitive and subdominant RAP-1-related antigen (RRA) is expressed by Babesia bovis merozoites. Parasitology, 138(7), 809–818. doi:10.1017/S0031182011000321 [PubMed: 21554842]

Swanson SJ, Neitzel D, Reed KD, & Belongia EA (2006). Coinfections acquired from Ixodes ticks. Clin Microbiol Rev, 19(4), 708–727. doi:10.1128/CMR.00011-06 [PubMed: 17041141]

Takayama K, Rothenberg RJ, & Barbour AG (1987). Absence of lipopolysaccharide in the Lyme disease spirochete, Borrelia burgdorferi. Infect Immun, 55(9), 2311–2313. doi:10.1128/IAI.55.9.2311-2313.1987 [PubMed: 3623705]

Takeuchi O, & Akira S (2010). Pattern recognition receptors and inflammation. Cell, 140(6), 805–820. doi:10.1016/j.cell.2010.01.022 [PubMed: 20303872]

Thekkiniath J, Kilian N, Lawres L, Gewirtz MA, Graham MM, Liu X, … Ben Mamoun C (2019). Evidence for vesicle-mediated antigen export by the human pathogen Babesia microti. Life Sci Alliance, 2(3). doi:10.26508/lsa.201900382

Thekkiniath J, Mootien S, Lawres L, Perrin BA, Gewirtz M, Krause PJ, … Ben Mamoun C (2018). BmGPAC, an Antigen Capture Assay for Detection of Active Babesia microti Infection. J Clin Microbiol, 56(10). doi:10.1128/JCM.00067-18

Tomasiewicz K, Chmielewska-Badora J, Zwolinski J, & Murias-Brylowska E (2016). Analysis of main T-cell subsets and activated T supressor/cytotoxic cells in patients with Borrelia burgdorferi s. lato only infection and co-infections with Anaplasma phagocytophilum, Bartonella spp. and Babesia microti. Ann Agric Environ Med, 23(1), 111–115. doi:10.5604/12321966.1196864 [PubMed: 27007527]

Totemeyer S, Foster N, Kaiser P, Maskell DJ, & Bryant CE (2003). Toll-like receptor expression in C3H/HeN and C3H/HeJ mice during Salmonella enterica serovar Typhimurium infection. Infect Immun, 71(11), 6653–6657. doi:10.1128/iai.71.11.6653-6657.2003 [PubMed: 14573691]

Vannier E, Borggraefe I, Telford SR, Menon S, Brauns T, Spielman A, … Wortis HH (2004). Age-associated decline in resistance to Babesia microti is genetically determined. Journal of Infectious Diseases, 189(9), 1721–1728. doi:Doi 10.1086/382965

Wang G, Ojaimi C, Iyer R, Saksenberg V, McClain SA, Wormser GP, & Schwartz I (2001). Impact of genotypic variation of Borrelia burgdorferi sensu stricto on kinetics of dissemination and severity of disease in C3H/HeJ mice. Infection and Immunity, 69(7), 4303–4312. doi:Doi 10.1128/Iai.69.7.4303-4312.2001 [PubMed: 11401967]

Wang Y, Su L, Morin MD, Jones BT, Whitby LR, Surakattula MM, … Beutler B (2016). TLR4/MD-2 activation by a synthetic agonist with no similarity to LPS. Proc Natl Acad Sci U S A, 113(7), E884–893. doi:10.1073/pnas.1525639113 [PubMed: 26831104]

Wells CA, Ravasi T, Faulkner GJ, Carninci P, Okazaki Y, Hayashizaki Y, … Hume DA (2003). Genetic control of the innate immune response. BMC Immunol, 4, 5. doi:10.1186/1471-2172-4-5 [PubMed: 12826024]

Werling D, & Jungi TW (2003). TOLL-like receptors linking innate and adaptive immune response. Vet Immunol Immunopathol, 91(1), 1–12. [PubMed: 12507844]

Wooten RM, Ma Y, Yoder RA, Brown JP, Weis JH, Zachary JF, … Weis JJ (2002a). Toll-like receptor 2 is required for innate, but not acquired, host defense to *Borrelia burgdorferi*. J Immunol, 168(1), 348–355. [PubMed: 11751980]

Wooten RM, Ma Y, Yoder RA, Brown JP, Weis JH, Zachary JF, … Weis JJ (2002b). Toll-like receptor 2 plays a pivotal role in host defense and inflammatory response to Borrelia burgdorferi. Vector Borne Zoonotic Dis, 2(4), 275–278. doi:10.1089/153036602321653860 [PubMed: 12804169]

Wooten RM, & Weis JJ (2001). Host-pathogen interactions promoting inflammatory Lyme arthritis: use of mouse models for dissection of disease processes. Curr Opin Microbiol, 4(3), 274–279. [PubMed: 11378478]

Take Aways

Live imaging allows detection of Lyme spirochetes colonization in different organs at different stages of infection of mice. Exacerbation of TLR2 signaling by *B. burgdorferi* and inflammation occurs during co-infection with *B. microti* in TLR4-defective host. *B. microti* PAMPs including its GPI anchor on merozoites surface fail to signal host cells through TLR2/TLR4.
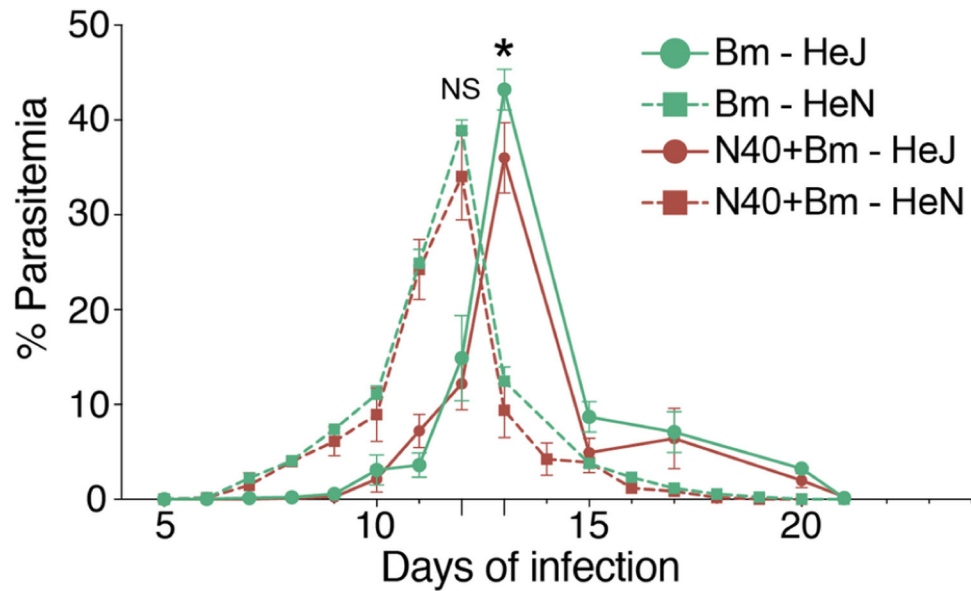
Figure 1. TLR4 deficiency prolongs survival of *B microti* in mouse blood.

Parasitemia determined in ten C3H/HeJ and C3H/HeN mice infected with *Bm* (10^4 infected erythrocytes injected i.p.) alone, or together with *B. burgdorferi* (10^3 spirochetes injected s.c. per mouse) by microscopic examination of Giemsa-stained thin blood smears at regular intervals. Each point represents average parasitemia in each group of mice (mean ± s.d.) with peak parasitemia significantly higher (p<0.05) in *Bm* infected than in respective co-infected mouse strain but not significantly different between C3H/HeJ and C3H/HeN mice due to each infection (NS). Onset of parasitemia in *Bm* infected and co-infected C3H/HeN appeared earlier than in C3H/HeJ mice (7th versus 10th day post-infection) but it cleared slightly faster (on 19th and 18th day of infection, respectively) than that in C3H/HeJ mice in which parasitemia was detectable in both *Bm* infected and co-infected mice until 20th day post-infection.
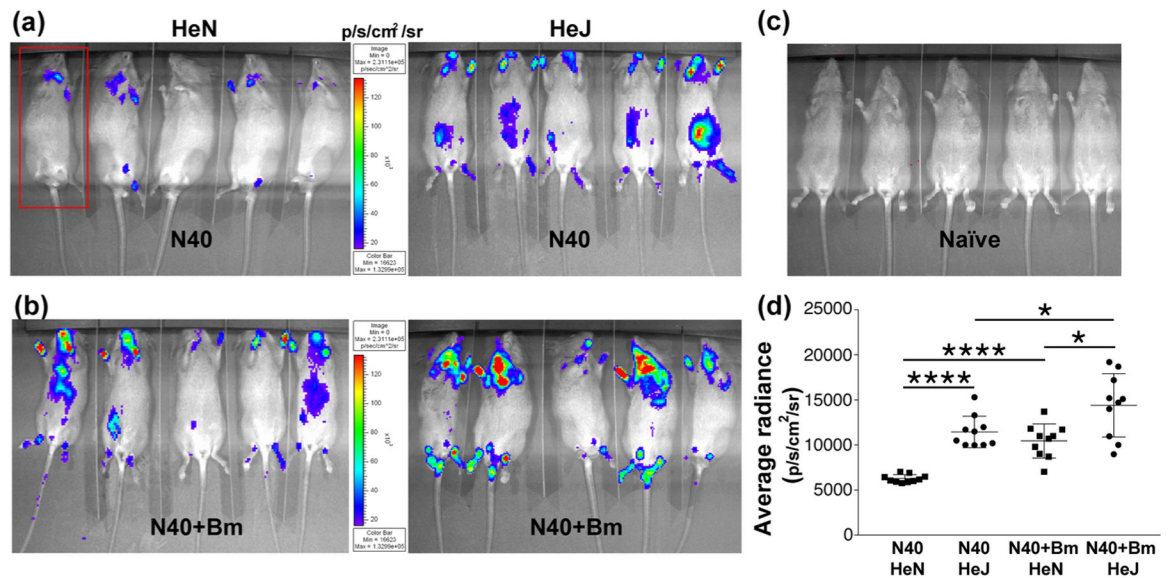
Figure 2. Colonization of organs by *B. burgdorferi* in C3H/HeJ and C3H/HeN mice infected with N40 alone and co-infected with *Bm* at two weeks of infection.
(a) Representative real-time images of five C3H/HeJ (HeJ) and C3H/HeN (HeN) mice infected with bioluminescent N40 strain using IVIS-200 displaying bioluminescence as a semi-quantitative indicator of *B. burgdorferi* colonization in different tissues of mice. Bioluminescence radiance in the whole body of each mouse (as marked in one mouse by a red rectangle) was also measured. **(b)** Overall, light emission in five mice each, representing colonization of organs and spirochetal burden in co-infected C3H/HeJ and C3H/HeN mice at two weeks post-infection. **(c)** A set of five uninfected mice was also imaged at the same time with average bioluminescence radiance measured to be (483.23 p/s/cm^2/sr). **(d)** Average bioluminescence radiance from five uninfected mice was deducted from the radiance obtained for each infected mouse (as marked in 2a and 2b) and net radiance values data for ten mice for each infection is presented. Horizontal lines indicate the net mean radiance in each group of infected mice. Statistical analysis was conducted using a two-tailed unpaired student t tests for unequal variance to determine significant difference between the paired groups (*p<0.05, ****p<0.0001).
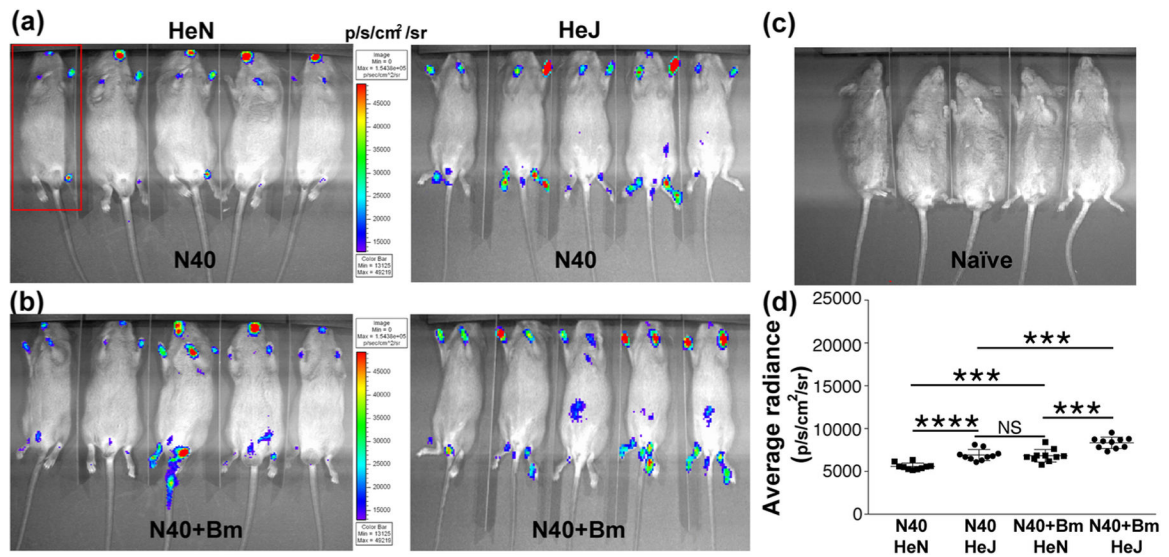
Figure 3. Colonization of mice organs by *B. burgdorferi* as detected by light emission due to the presence of live bioluminescent N40 strain at three weeks of infection.
(a) Representative real-time images of five C3H/HeJ (HeJ) and C3H/HeN (HeN) mice infected with bioluminescent N40 strain using IVIS-200 displaying bioluminescence in the head and joints regions. Bioluminescence radiance in the whole body of each mouse (as marked in one mouse by a red rectangle) was also measured. **(b)** Bioluminescence detection in co-infected C3H/HeJ and C3H/HeN mice. **(c)** Live imaging of a set of five uninfected mice at the same time point. **(d)** Average bioluminescence radiance from five uninfected mice was deducted from the radiance obtained for each infected mouse and net radiance data for each mouse is shown. Horizontal lines indicate the comparison of net mean radiance in each group of infected mice. Difference between average bioluminescence radiance in N40-infected C3H/HeJ and co-infected C3H/HeN mice was not statistically significant (NS). Statistical analysis was conducted using a two-tailed unpaired student t tests for unequal variance to determine significant difference between the paired groups (***p<0.001, ****p<0.0001).
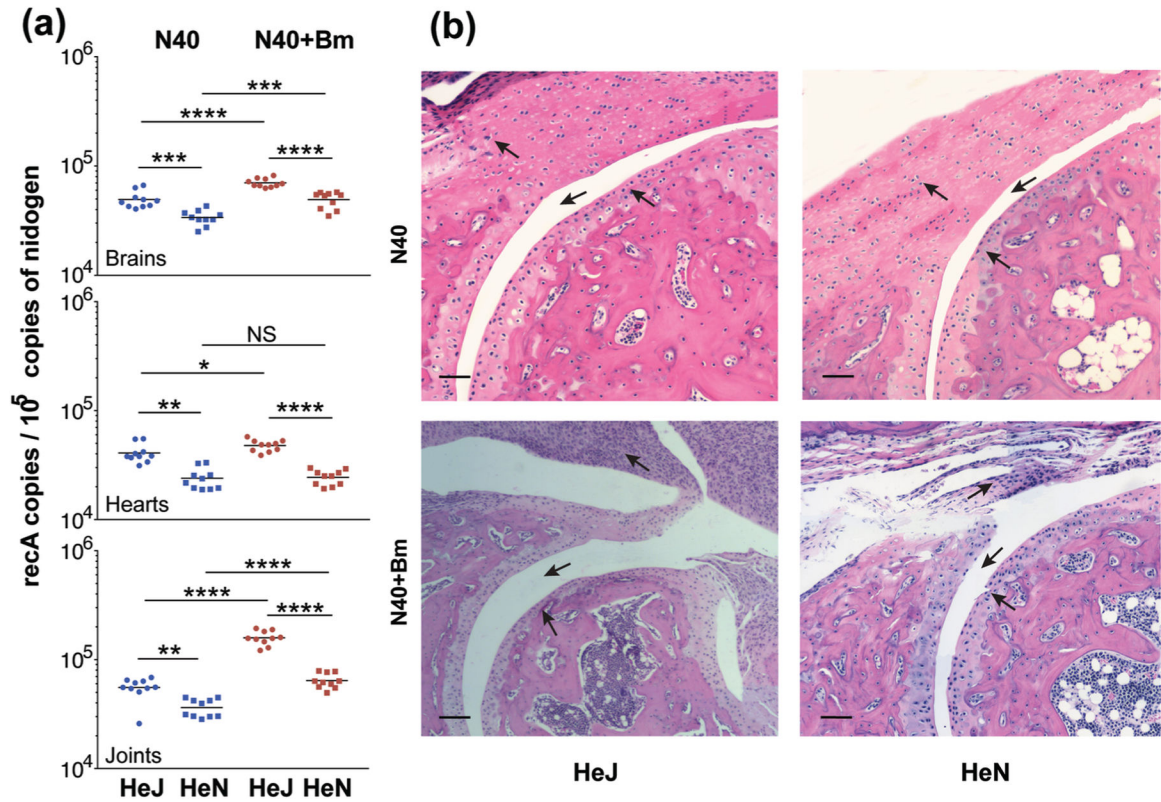
Figure 4. *B. burgdorferi* **strain N40 colonization levels determined by qPCR and resulting pathology in C3H/HeJ and C3H/HeN mice.**

(a) Burden of *B. burgdorferi* in tissues as detected by duplex qPCR assay from ten mice for each group using *recA* primers and molecular beacon probes with mouse nidogen amplicon copy number used for normalization of spirochete quantities. Horizontal lines represent the mean *B. burgdorferi recA* copy number per 10^5 copies of nidogen genes. Statistical analysis was conducted using a two-tailed unpaired student t tests for unequal variance to determine significant difference between the paired groups (NS-Not significant, *p<0.05, **p<0.01, ***p<0.001, ****p<0.0001). **(b)** Severe arthritis in tibiotarsal joint manifested by synovial hyperplasia and erosion of cartilage, higher lymphocytic infiltration and change in synovial space (arrows) were observed in co-infected mice as compared to *B. burgdorferi*-infected mice of both strains. Bar represents a size of 100μm.
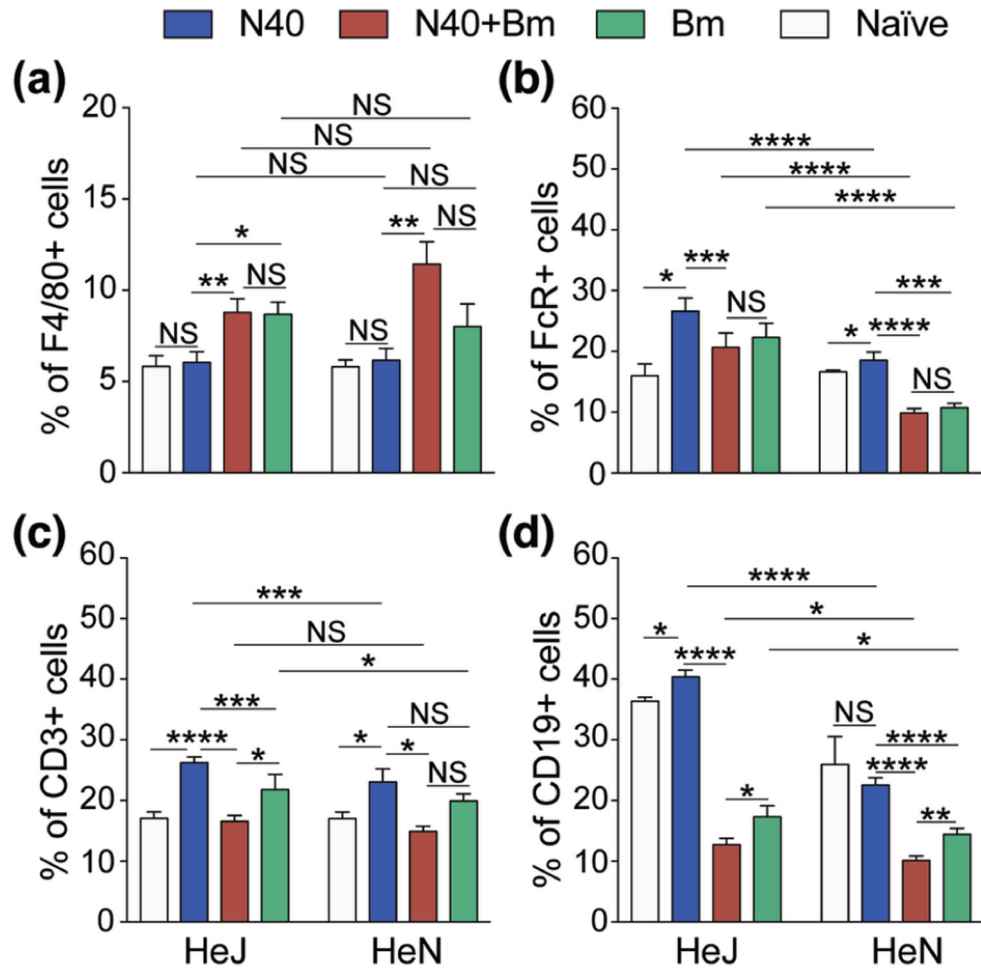
Figure 5. Modulation of splenic immune responses in mice by infection with *B microti* and N40 separately, or simultaneously.
(a) Single cell suspension of mice spleen infected with N40, *Bm* and N40 +*Bm* were prepared and stained with fluorophore-conjugated antibodies against F4/80+ (macrophages), **(b)** FcR+ phagocytic cells, **(c)** CD3+ (T cells), and **(d)** CD19+ (B cells), followed by FACS analysis. Higher percentages of B, FcR+ phagocytic and T cells were observed in C3H/HeJ mice. Proportions of various immune cells from spleens of mice from each experimental group analyzed by FACS are expressed as mean ± s.d. Statistical analysis was conducted using a two-tailed unpaired student t tests for unequal variance to determine significant difference between the paired groups (NS-Not Significant, *p<0.05, **p<0.01, ***p<001, ****p<0.0001).
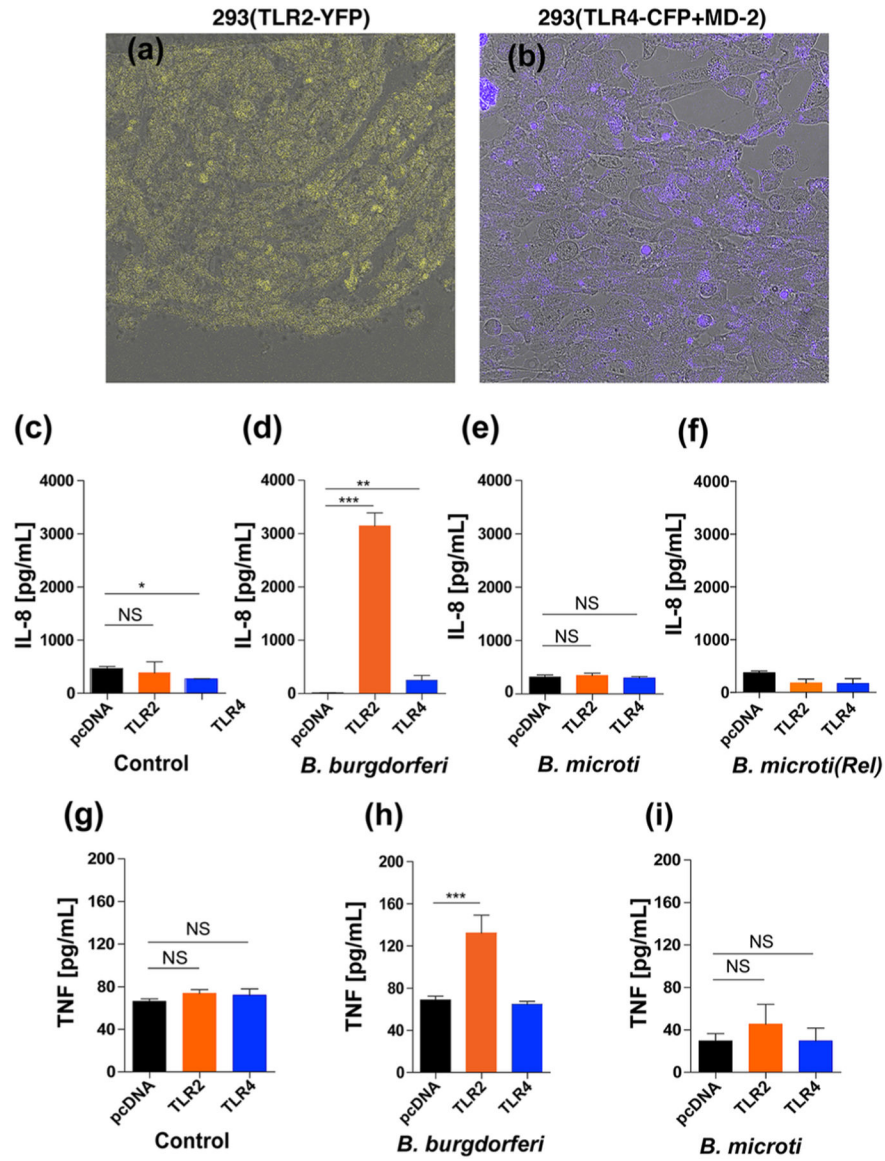
Figure 6. Response of TLR2/TLR4 transfected HEK293 cells to B. burgdorferi N40 strain and *Bm*-infected mouse blood.

(a and b) Yellow fluorescence and Cyan fluorescence associated with TLR2-YFP and TLR4-CFP+MD-2 transfected HEK293 cells confirmed expression of respective TLRs. **(c and d)** As compared to control (6c, medium only) treatment, exposure of transfected HEK293 cells to 2×10^7 *B. burgdorferi* for ~16h resulted in high stimulation of TLR2 and moderate but significant level of stimulation of TLR4 to produce pro-inflammatory IL-8 cytokine (6d). **(e and f)** Neither treatment with 1×10^6 RBCs of *Bm* infected mouse blood (~3.1×10^5 iRBCs) nor released (Rel) *Bm* parasites suspended in 20μg/ml Polymyxin B containing treatment medium stimulated TLR2 or TLR4 to produce pro-inflammatory IL-8 cytokine. **(g, h and i)** Significant TNF-α (TNF) stimulation was only observed by *B. burgdorferi* N40 strain treatment of HEK293 cells transfected with TLR2. Again, *Bm* did not shown stimulation neither of TLR2 nor TLR4 expressed in HEK293 cells. Statistical analysis was conducted using a two-tailed unpaired student t tests for unequal variance to

determine significant difference between the paired groups (NS-Not significant, *p<0.05, **p<0.01, ****p<0.0001).

Table 1.

Histopathological scoring of joints of infected mice

Experimental groups		Number* of mice with each inflammation score for joints							
		Knee			Tibiotarsus				
		−	+/−	+	−	+/−	+	++	+++
C3H/HeJ	*B. burgdorferi*	1	2	2	0	0	1	4	0
C3H/HeN	*B. burgdorferi*	2	1	2	0	0	3	1	1
C3H/HeJ	*B. burgdorferi* +Bm	1	0	4	0	0	0	3	2
C3H/HeN	*B. burgdorferi* +Bm	0	2	3	0	0	2	1	2
C3H/HeJ	*Bm*	5	0	0	5	0	0	0	0
C3H/HeN	*Bm*	2	2	0	4	0	0	0	0

* Numbers of infected mice in each group of 5 infected mice, except 4 *Bm* infected C3H/HeN mice that showed a specific inflammation score for knee and tibiotarsus. Inflammation scoring was based upon infiltration of lymphocytes in the synovium and perisynovium, hyperplasia of the synovium, erosion or cellular infiltration of articular cartilage, increased synovial space and the severity of the lesions was ranked on a scale from no inflammation (−) that is equivalent to uninfected mice, to maximum inflammation (+++).